Spectroscopy and Modelling of a High Power Diode-pumped 2.3 μm Yb:Tm:YLF Laser

N. U. Wetter, P. S. F. de Matos, L. Gomes, I. M. Ranieri, S. L. Baldochi
Centro de Lasers e Aplicações, IPEN/SP
Av. Prof. Lineu Prestes, 2242, São Paulo 05508-000 Brazil
nuwetter@ipen.br

Energy transfer processes in Yb:Tm:YLF under 960 nm pumping have been quantitatively studied and a computer simulation considering the full rate-equation scheme has been performed. The 2.3 μm laser achieved 620 mW of output power.

OCIS codes: (140.3480) Lasers, diode-pumped; (300.6360) Spectroscopy, laser

1. Introduction

Lasers emitting around 2.3 μm are important in many application as in gas detection systems [1,2] and LIDAR applications [3]. Recently, lasers in the region 2.0-2.5 μm have gained renewed interest for noninvasive blood glucose measurements [4] because of their capability to generate measurements with very high signal-to-noise ratio. In the YLF host, thulium has a large emission spectra around 2.3 μm and strong absorption lines at 685 and 780 nm that are accessible with diode lasers [5]. Due to a highly concentration dependent cross-relaxation process that leads to a reduction of the 2.3 micron emission from the upper laser level, the thulium concentration should be kept below 2 mol % [5]. For efficient pump absorption, a highly concentrated sensitizer can be used, such as Ytterbium that can be diode-pumped at 960 nm where high-power diodes are available.

In the 960 nm Yb:Tm pumping scheme occur three (K_1,K_2,K_3) energy transfer up-conversion processes (ETU) as illustrated in figure 1. After pump excitation from the $^2F_{7/2}$ level to the $^2F_{5/2}$ level, the first ETU process K_1 transfers energy from the ytterbium to the $^3H_5$ thulium level, followed by a fast multi-phonon relaxation down to the $^3F_4$ level. The second ETU process, K_2, to the $^3F_2$ energy level of Tm^{3+} is followed by a rapid relaxation and populates the upper laser level ($^3H_4$). The third ETU, K_3, causes losses to the system because it transfers population from the upper laser level into the $^1G_4$ level of Tm. Other processes deplete the upper laser level: the cross-relaxation originating from the $^3H_4$ and $^3H_6$ levels to the $^3F_4$ level (K_4) and the back-transfer (K_5) from the $^3H_4$ thulium level to $^2F_{5/2}$ ytterbium level. Laser action at 2.3 micron in Tm is based on the $^3H_4$-$^3H_5$ transition.

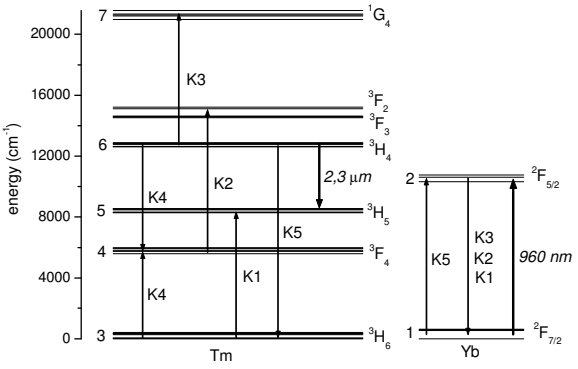

Fig. 1: Energy-level scheme of Yb:Tm:YLF. K_1, K_2, K_3 represent energy transfer upconversions; K_4 is a cross-relaxation and K_5 a back-transfer.

2. Spectroscopy

The energy transfer rates and concentration dependent lifetimes were measured by pumping with an OPO which delivers a typical energy of 10 mJ with a repetition rate of 10 Hz, pulse duration of 4 ns and bandwidth of 4 nm into a focal spot of radius 0.3 mm. The detection apparatus consisted of a single grating spectrometer, a refrigerated photomultiplier for the visible and an InSb detector refrigerated at liquid nitrogen temperature. To measure the $^3F_4$ emission, the Yb:Tm:YLF crystal was excited at 960 nm and the thulium emission was collected at 1900 nm. Care

was taken to avoid radiation trapping by exciting the sample at the edge closest to the detection apparatus. As seen in figure 2a), the measurements and the applied fit are in good agreement. The calculated rise time t_s is 0.807±0.062 ms and the decay time is 15.04±0.12 ms which is in good agreement with other authors [6]. Using an intrinsic decay time of τ = 2.1 ms for the ytterbium $^2F_{5/2}$ level [7], we calculate a probability of K_1 of 776 s^{-1}. The second step energy-transfer process involves two donors, the ytterbium $^2F_{5/2}$ and the thulium $^3F_4$ energy-levels. The transfer rate K_2 depends on the first-step energy-transfer rate K_1. In order to calculate K_2 we measured the $^3H_4$ fluorescence emission at 800 nm. The combined rise time was measured to be 0.650±0.017 ms ($K=1538 s^{-1}$). Using $K = (K_1 \cdot K_2)^{0.5}$ we obtain K_2 = 1489 s^{-1}.

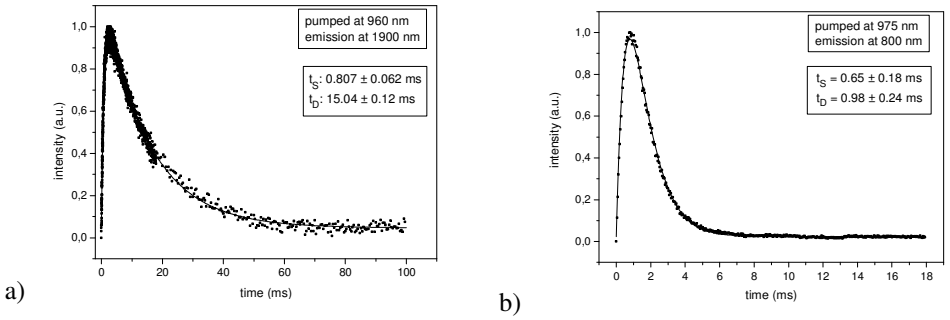

Fig. 2: a) Thulium emission at 1900 nm. Inset shows the fitted rise time for the first Yb-Tm energy transfer and lifetime of the thulium $^3F_4$ level. Pump wavelength was 960 nm. b) Thulium emission from the $^3H_4$ energy level measured at 800 nm. Inset shows the second-step-ETU rise time and the decay time of the laser level. Pump wavelength was 975 nm.

3. Simulation and experiment

We used a numerical, time resolved simulation which included all energy-levels of figure 1. The system of eight differential, non-linear equations is solved using a fourth order Runge-Kutta algorithm. Pump power and output power measurements were done with a calibrated power meter of 10 mW resolution. Diode emission spectra were recorded with a portable spectrometer, coupled to a PC and crystal absorption and emission spectra were recorded with a high-resolution spectrometer. The temporal behavior of the output pulse was analyzed with a thermoelectrically cooled, fast rise time InAs detector. Care was taken to attenuate the pulses in order to avoid saturation effects of the detector. Laser experiments were done with a 14 W, 960 nm diode bar that was focused to a spot size of 0.2x0.4 mm^2 at the Brewster cut crystal of 4.6 mm length inside the hemispherical cavity of 1% output transmission. The rate equations for the populations densities n_i and the photon density ϕ are given in table 1.

Table 1: Equations and parameters used in the model. Branching ratios, τ_5 and τ_7 are from [6], K_4 and K_5 from [8].

$$\frac{dn_1}{dt} = -R_{12} + \frac{n_2}{\tau_2} + K_1 n_2 n_3 + K_2 n_2 n_4 + K_3 n_2 n_6 - K_5 n_1 n_6$$

$$\frac{dn_2}{dt} = R_{12} - \frac{n_2}{\tau_2} - K_1 n_2 n_3 - K_2 n_2 n_4 - K_3 n_2 n_6 + K_5 n_1 n_6$$

$$\frac{dn_3}{dt} = + \frac{n_4}{\tau_4} + \frac{\beta_{63} n_6}{\tau_6} + \frac{\beta_{73} n_7}{\tau_7} - K_1 n_2 n_3 - K_4 n_3 n_6 + K_5 n_1 n_6$$

$$\frac{dn_4}{dt} = - \frac{n_4}{\tau_4} + \frac{n_5}{\tau_5} + \frac{\beta_{64} n_6}{\tau_6} + \frac{\beta_{74} n_7}{\tau_7} - K_2 n_2 n_4 + 2K_4 n_3 n_6$$

$$\frac{dn_5}{dt} = R_{SE} - \frac{n_5}{\tau_5} + \frac{\beta_{65} n_6}{\tau_6} + \frac{\beta_{75} n_7}{\tau_7} + K_1 n_2 n_3$$

$$\frac{dn_6}{dt} = -R_{SE} - \frac{n_6}{\tau_6} + \frac{\beta_{76} n_7}{\tau_7} + K_2 n_2 n_4 - K_3 n_2 n_6 - K_4 n_3 n_6 - K_5 n_1 n_6$$

$$\frac{dn_7}{dt} = - \frac{n_7}{\tau_7} + K_3 n_2 n_6$$

$$\frac{d\phi}{dt} = \frac{L_{cr} c N_{Tm}}{L_{cav}} \left(R_{SE} + f \frac{n_6}{\tau_6} \right) + \frac{\ln(R_{out} T) c \phi}{2 L_{cav}}$$

τ_2	2 ms
τ_4	15 ms
τ_5	1 µs
τ_6	1 ms
τ_7	0.54 ms
β_{63}	0.924
β_{73}	0.406
β_{64}	0.07
β_{74}	0.076
β_{65}	0.006
β_{75}	0.366
β_{76}	0.155

K_1	776 s^{-1}
K_2	1489 s^{-1}
K_3	5094 s^{-1}
K_4	500 s^{-1}
K_5	210 s^{-1}
σ_{12}	$7x10^{-21}$ cm^2
σ_{65}	$1.2x10^{-20}$ cm^2
N_{Tm}	$1.6x10^{20}$ cm^{-3}
N_{Yb}	$13.4x10^{20}$ cm^{-3}
f	10^{-7}
L_{cav}	2.3 cm

where the energy levels are labeled as in figure 1. σ_{65} is the laser emission cross section, β_{ij} are the branching ratios, N_{Tm} and N_{Yb} the dopant and sensitizer concentrations, respectively, f is the fraction of spontaneously emitted photons coupled into the laser mode and R_{se} is the stimulated emission rate given by $R_{se}=(b_6n_6 - 0.5b_5n_5)\sigma_{65}\phi$. The pump rate is calculated by $R_{12}=I\eta n_1\sigma_{12}$, where η is the pump delivery efficiency and I is the pump flux. The effective pump absorption cross-section, σ_{12}, is given by the overlap of the normalized diode emission spectra and the crystal absorption spectra, integrated over the crystal length.

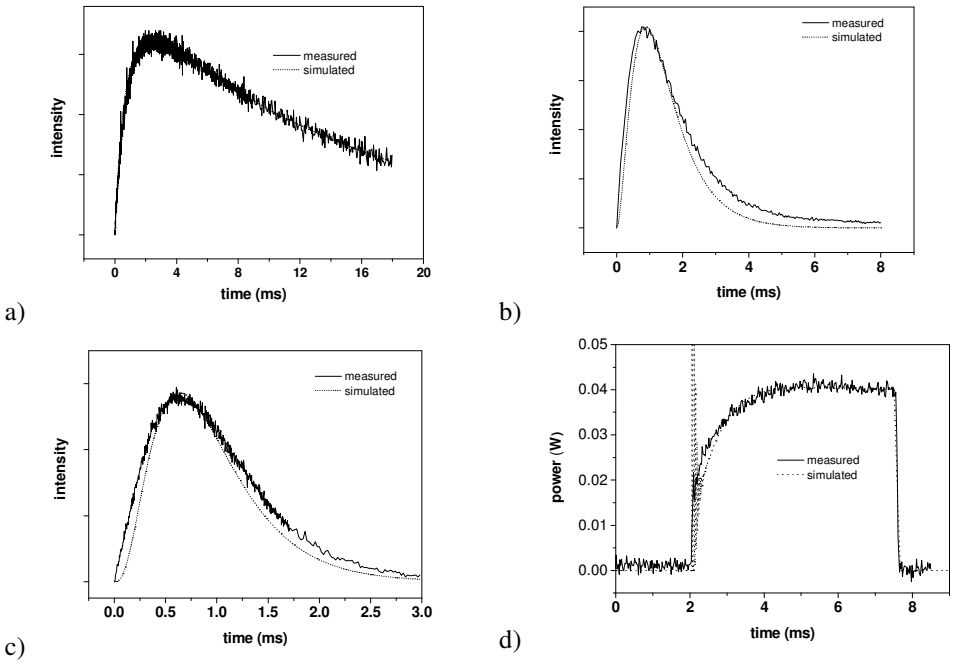

Fig. 3: a),b),c) Measured and simulated decay curves of the $^3F_4$, $^3H_4$ and $^1G_4$ levels, respectively. d) measured and simulated output power curve obtained at low pump power (5 W).

3. Results

Maximum output power was 620 mW in qcw operation using pump pulses of P = 14 W and pulse duration of 8 ms. In pure cw operation we achieved approximately 400 mW before the crystal was damaged. As seen in figure 3, we achieved excellent agreement between our model and the obtained experimental data, using the above measured decay rates. Output power, pulse delay and decay time are also in good agreement with simulations except at high pump powers where we observed a mismatch at the pulses leading edge which is probably due to higher order effects not taken into account by our model.

4. References

[1] F. J. McAleavey, J. O'Gorman, J. F. Donegan, J. Hegarty and G. Maze, "Extremely high sensitivity gas detection at 2.3 μm using a grazing incidence Tm^{3+} fibre laser cavity", Sensors and Actuators A **87**, 107-112 (2001).
[2] L. Cerutti, A. Garnache, A. Ouvrard, M. Garcia and F. Genty, "Vertical cavity surface emitting laser sources for gas detection", Phys. Stat. Sol. A **2002** (4), 631-635 (2005).
[3] M. E. Webber, J. Wang, S. T. Sanders, D. S. Baer, R. K. Hanson. In situ combustion measurements of CO, CO2, H2O and temperature using diode laser absorption sensors. Proceedings Of The Combustion Institute 28: 407-413 Part 1 (2000).
[4] J. T. Olesberg C. Mermelstein, J. Schmitz and J. Wagner, "Tunable laser diode system for noninvasive blood glucose measurements" in Optical Diagnostics and Sensing V , A. V. Priezzhev and G. L. Cote, eds, Proc. SPIE 5702, 23-29 (2005).
[5] J. F. Pinto, L. Esterowitz, G. H. Rosenblatt, "Tm^{3+}:YLF laser continuously tunable between 2.20 and 2.46 μm", Opt. Lett. **19** (12), 683-685 (1994).
[6] I. K. Razumova, A. M. Tkachuk, D. I. Mironov, A. A. Nikichev, "Spectral intensities and stimulated radiation of Tm3+:YLF crystals", Opt. Spectr. **81** (2), 205-213 (1996).
[7] L. D. De Loach *et al*, "Evaluation of absorption and emission properties of Yb^{3+} doped crystals for laser applications", IEEE J. Quantum Electron. **29** (4), 1179-1191 (1993).
[8] A. Diming, P. E. A. Mobert, G. Huber, "Diode-pumped continuous wave, quasi continuous wave and q-switched laser operation of Yb^{3+}, tm^{3+}:$YLiF_4$ at 1.5 and 2.3 μm," J. Appl. Phys. **84**(11), 5900-5904 (1998).